JOC Article

2,7-Substituted Hexafluoroheterofluorenes as Potential Building Blocks for Electron Transporting Materials

Katharine Geramita, Jennifer McBee, and T. Don Tilley*

Department of Chemistry, University of California at Berkeley, Berkeley, California 94720

tdtilley@berkeley.edu

Received September 28, 2008

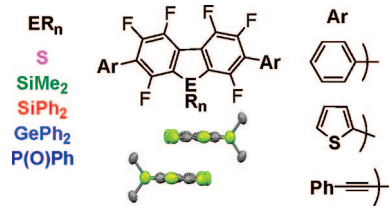

A series of 2,7-substituted hexafluoro-9-heterofluorenes was synthesized via nucleophilic aromatic substitution (S_NAr_F) reactions of phenyllithium, thienyllithium, and lithium phenylacetylide with various octafluoroheterofluorenes and 2,2′-dibromooctafluorobiphenyl. These compounds are of interest as possible building blocks for materials with useful electron transport properties, since they possess relatively low LUMO energy levels. The HOMO−LUMO energy gaps, as determined by UV−vis spectroscopy, range between 3.0 and 3.9 eV, while photoluminescence emission spectra reveal λ_{ems} values in the range of 365 to 420 nm (corresponding to ultraviolet to violet/blue emission). Dilute solution state quantum yields vary significantly with the nature of the heteroatom and the 2,7-substituents, and approach unity for a number of the di(phenylethynyl) derivatives. The experimentally determined LUMO energy levels (−2.7 to −3.3 eV as determined by differential pulse voltammetry) suggest that these compounds may be good candidates for electron transport applications. Single-crystal X-ray analyses of a number of compounds revealed cofacial packing in all cases, with intermolecular distances as short as 3.4 Å.

Introduction

The use of organic semiconducting materials for applications in "plastic electronics", such as field effect transistors (FETs), organic light emitting diodes (OLEDs), and photovoltaics (PVs), continues to attract considerable interest.[1] Organic systems offer the possibility for cheap raw materials and low processing costs, and are readily tailored to access a wide range of physical, optical, and electrical properties in the final device.[1−4] In general, conjugated organic π-systems are effective hole-transporting (p-type) materials;[5] however, the development of improved devices (e.g., FET and PV) should be facilitated by the introduction of efficient electron-conducting (n-type) materials.[4,6]

Useful n-type organic materials possess a low barrier to electron injection and effectively transport a negative charge. While it is generally accepted that a low-energy LUMO should facilitate charge injection, the attributes that contribute to high electron mobility are not well understood.[7] Electron-deficient π-systems are thought to be associated with high electron mobility, and pyridines, oxadiazoles, perylene diimides, metalloles, and fluorinated aromatics have been identified as potential n-type materials.[8−13] Additionally, close cofacial intermolecular packing has been associated with increased charge transport in a number of organic systems.[14] Therefore, molecular organic building blocks that contain an electron-deficient, extended π-system, a stabilized LUMO, and close cofacial stacking in the solid state would be of great interest to the development of this field.

(1) (a) Forrest, S. R. *Chem. Rev.* **1997**, *97*, 1793. (b) Jenekhe, S. *Chem. Mater.* **2004**, *16* (23), 4382 (special issue on organic electronics). (c) Forrest, S. R.; Thompson, M. E. *Chem. Rev.* **2007**, *107* (4), 923 (special issue on organic electronics).

(2) Hwang, D. H.; Kim, S. K.; Park, M. J.; Koo, B. W.; Kang, I. N.; Kim, S. H.; Zyung, T. *Chem. Mater.* **2004**, *16*, 1298.

(3) Schwartz, M.; Srinivas, G.; Yeates, A.; Berry, R.; Dudia, D. *Synth. Met.* **2004**, *143*, 229.

(4) Zhu, Y.; Alam, M. M.; Jenekhe, S. A. *Macromolecules* **2003**, *36*, 8958.

(5) Renak, M. L.; Bartholomew, G. P.; Wang, S. J.; Ricatto, P. J.; Lachicotte, R. J.; Bazan, G. C. *J. Am. Chem. Soc.* **1999**, *121*, 7787.

(6) Tonzola, C. J.; Alam, M. M.; Kaminsky, W.; Jenekhe, S. A. *J. Am. Chem. Soc.* **2003**, *125*, 13548.

(7) (a) Chua, L.-L.; Zaumseil, J.; Chang, J.-F.; Ou, E.; Ho, P.; Sirringhaus, H.; Friend, R. *Nature* **2005**, *434*, 194. (b) Zaumseil, J.; Sirringhaus, H. *Chem. Rev.* **2007**, *107*, 1296.

10.1021/jo802171t CCC: $40.75
Published on Web 12/09/2008

Metalloles, which are five-membered heterocycles containing a heteroatom and a diene moiety, are associated with low-energy LUMO levels, resulting from the stabilization of the diene π-system via interaction with the heteroatom-based σ^* oribtals.[15,16] The LUMO energy level is generally unaffected by minor variations in the R groups on the heteroatom (vida infra), which can be changed to modify solubility and packing properties. Siloles in particular have exhibited exceptionally good performance in OLED devices but often exhibit poor intermolecular cofacial interactions due to the orientation of the aryl groups that usually occupy the 3- and 4-positions.[10a,17,18] The analogous sulfur (thiophene) and phosphorus (phosphole)-based systems have shown great promise in a number of electronic applications.[16] Often thiophene- and phosphole-based systems function as hole transporting materials; however, it is possible that their incorporation into the highly electron-deficient perfluorofluorene framework might afford interesting n-type compounds. Additionally, the related phosphole oxide derivatives possess a more electron-deficient π-system and should afford compounds with high electron affinities.

Compounds containing the dibenzometallole (or metallofluorene) fragment are interesting candidates for n-type materials, since they possess a planar aromatic structure while maintaining the LUMO-lowering ability of the metallole fragment. In general fluorene-based systems are electron rich and tend to pack in a herringbone structure.[19−21] However, fluorine atom substituents in the aromatic system may improve both electron transport and cofacial packing.[12,13,22,23] Previous work in our laboratories on the synthesis and characterization on 2,7-bis(pentafluorophenylethynyl)hexafluoro-9-heterofluorenes has demonstrated that these systems pack with parallel heterofluorene fragments and possess stabilized LUMO energy levels.[24] Additional work in our laboratories has demonstrated that nucleophilic aromatic substitution (S_NAr_F) is a highly effective method for carbon−carbon bond formation involving perfluoroaromatic compounds, and high conversion to a single product was observed for a variety of substrates.[10a,24,25] In this report we describe the synthesis and physical, optical, and electrochemical characterization of a variety of 2,7-substituted hexafluoroheterofluorenes (Chart 1), prepared via nucleophilic aromatic substitution (S_NAr_F). The synthesis and characterization of these electron-deficient compounds greatly expands this class of 2,7-substituted hexafluoroheterofluorenes beyond the more highly fluorinated 2,7-bis(pentafluorophenylethynyl)hexafluoroheterofluorenes previously communicated.[24]

CHART 1

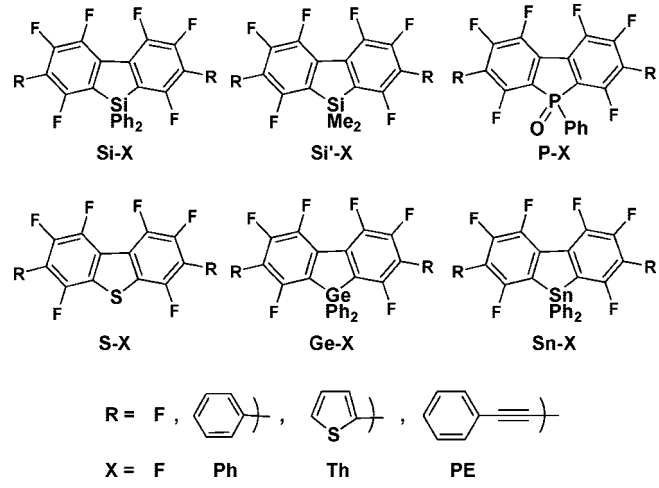

SCHEME 1

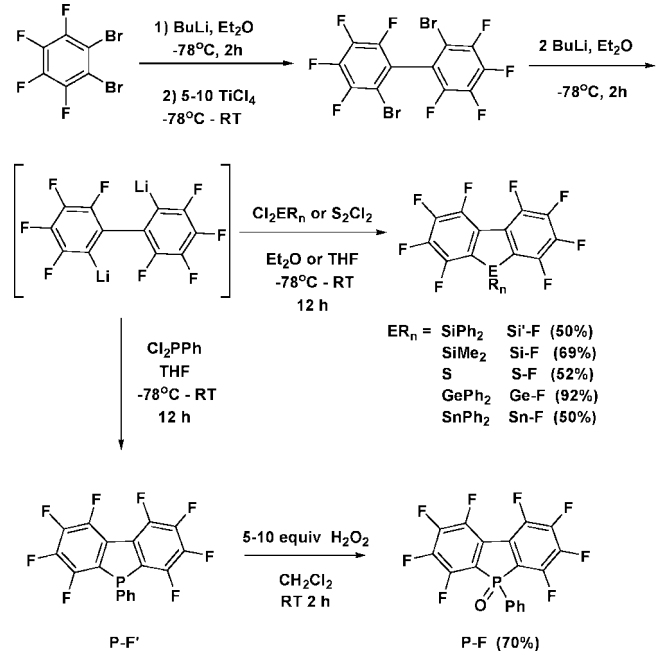

Results and Discussion

Synthesis of Fluorinated Heterofluorenes. The synthesis of octafluoroheterofluorenes (Scheme 1) from 1,2-dibromotetrafluorobenzene followed procedures slightly modified from those of

(8) Kulkarni, A.; Tonzola, C.; Babel, A.; Jenekhe, S. *Chem. Mater.* **2004**, *16*, 4556.
(9) Babudri, F.; Farinola, G.; Naso, F.; Ragni, R. *Chem. Commun.* **2007**, *10*, 1003.
(10) (a) Geramita, K.; McBee, J.; Shen, Y.; Radu, N.; Tilley, T. D. *Chem. Mater.* **2006**, *18*, 3261. (b) Tannaci, J. F.; Noji, M.; McBee, J.; Tilley, T. D. *J. Org. Chem.* **2007**, *72*, 5567.
(11) Tamao, K.; Uchinda, M.; Izumizawa, T.; Furukawa, K.; Yamaguchi, S. *J. Am. Chem. Soc.* **1996**, *118*, 11974.
(12) Facchetti, A.; Yoon, M. H.; Stern, C. L.; Katz, H. E.; Marks, T. J. *Angew. Chem., Int. Ed.* **2003**, *42*, 3900.
(13) Heidenhain, S. B.; Sakamoto, Y.; Suzuki, T.; Miura, A.; Fujikawa, H.; Mori, T.; Tokito, S.; Taga, T. *J. Am. Chem. Soc.* **2000**, *122*, 10240.
(14) Hutchison, G.; Ratner, M.; Marks, T. *J. Am. Chem. Soc.* **2005**, *127*, 16866.
(15) (a) Tamao, K.; Yamaguchi, S.; Shiro, M. *J. Am. Chem. Soc.* **1994**, *116*, 11715. (b) Yamaguchi, S.; Tamao, K. *J. Chem. Soc., Dalton Trans.* **1998**, 3693.
(16) (a) Hissler, M.; Dyer, P. W.; Reau, R. *Coord. Chem. Rev.* **2003**, *244*, 1. (b) Bumgartner, T.; Reau, R. *Chem. Rev.* **2006**, *106*, 4681.
(17) Murata, H.; Malliaras, G. G.; Uchida, M.; Shen, Y.; Kafafi, Z. H. *Chem. Phys. Lett.* **2001**, *339*, 161.
(18) (a) Luo, J.; Xie, Z.; Lam, J.; Cheng, L.; Chen., H.; Qui, C.; Kwok, H.; Zhan, X.; Lui, Y.; Zhu, D.; Tang, B. Z. *Chem. Commun.* **2001**, 1740. (b) Boydston, A. J.; Yin, Y.; Pagenkopf, B. L. *J. Am. Chem. Soc.* **2004**, *126*, 3724.
(19) (a) Rathnayake, H.; Cirpan, A.; Lahti, P.; Karasz, F. *J. Am. Chem. Soc.* **2006**, *18*, 560. (b) Heeney, M.; Bailey, C.; Giles, M.; Shkunov, M.; Sparrowe, D.; Tierney, S.; Zhang, W.; McCulloch, I. *Macromolecules* **2004**, *37*, 5250.
(20) Chen, C.-H.; Shen, W.-J.; Jakka, K.; Shu, C.-F. *Synth. Met.* **2004**, *143*, 215.
(21) Coropceanu, V.; Nakano, T.; Gruhn, N.; Kwon, O.; Yade, T.; Katsukawa, K.; Bredas, J.-L. *J. Phys. Chem. B* **2006**, *110*, 9482.
(22) Facchetti, A.; Yoon, M.-H.; Stern, C. L.; Hutchison, G. R.; Ratner, M. A.; Marks, T. J. *J. Am. Chem. Soc.* **2004**, *126*, 13859.
(23) (a) Gierschner, J.; Ehni, M.; Egelhaaf, H.-J.; Medina, B. M.; Beljonne, D.; Benmansour, H.; Bazan, G. *J. Chem. Phys.* **2005**, *123*, 144914. (b) Cho, D.; Parkin, S.; Watson, M. *Org. Lett.* **2005**, *7*, 1067. (c) Sakamoto, Y.; Komatsu, S.; Suzuki, T. *J. Am. Chem. Soc.* **2001**, *123*, 4643.
(24) Geramita, K.; McBee, J.; Tao, Y.; Segalman, R. A.; Tilley, T. D. *Chem. Commun.* **2008**, 5107.
(25) Nitschke, J.; Tilley, T. D. *J. Am. Chem. Soc.* **2001**, *123*, 10183.

SCHEME 2

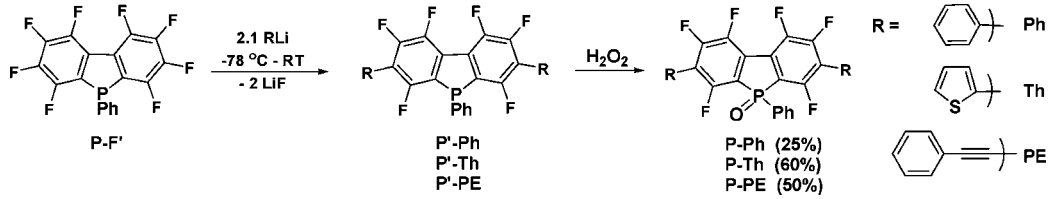

SCHEME 3

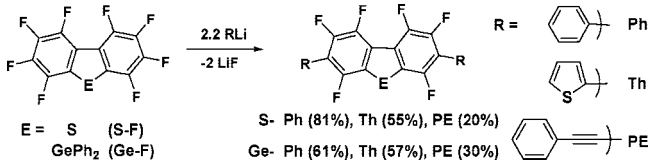

SCHEME 4

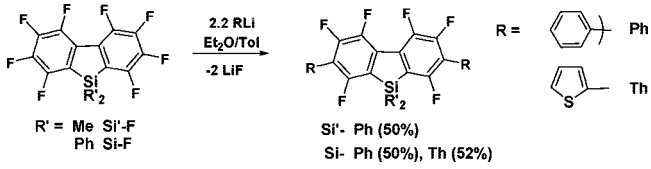

SCHEME 5

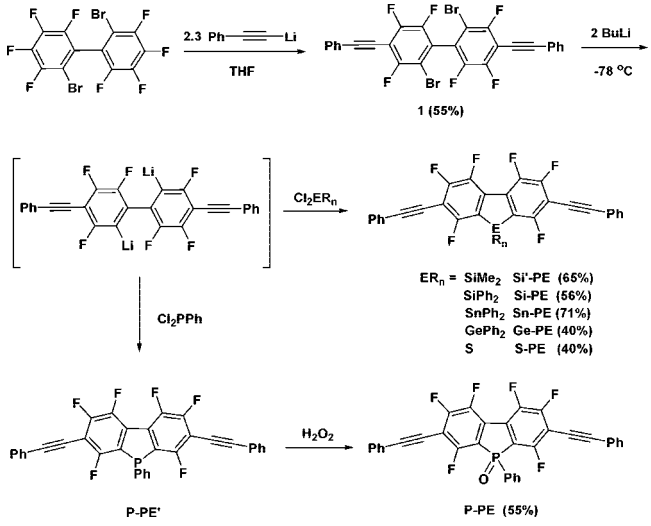

Cohen et al. (**Si-F**, **Si′-F**, **Ge-F**, **Sn-F**)[26] and Chambers et al. (**P-F**).[27] Their syntheses were previously reported to give low to moderate yields, but the methods have now been optimized to give the products in 50−90% yield. Additionally, it was possible to use this method to synthesize octafluorothiafluorene (**S-F**), which had previously been synthesized by a copper-mediated coupling of $S(2\text{-Br-}C_6F_4)_2$.[28] X-ray crystal structures (vide infra) were determined for octafluoroheterofluorenes containing silicon (**Si-F**, **Si′-F**), germanium (**Ge-F**), and tin (**Sn-F**).

All 2,7-substituted hexafluoroheterofluorenes were synthesized via nucleophilic aromatic substitution (S_NAr_F) under relatively mild reaction conditions (Schemes 2−5). Fluorinated arenes are good substrates for this carbon−carbon bond-forming method, which takes advantage of the electron-deficient nature of the aromatic system and the electronegativity of the fluorine atom.[10a,24,29] Control over the position of substitution can present a challenge for synthetic applications of S_NAr_F. It is well-established that the position of substitution is dictated by the stability of the anionic intermediate, whose dominant resonance structure is that with the negative charge localized in the position *para* to substitution, as illustrated for octafluoroheterofluorenes in eq 1.[30−32] While the relative stabilities of possible intermediates are easy to predict for simple perfluorinated arenes, such as decafluorobiphenyl or octafluoronaphthlanene, the situation is more complex for substituted fluoroarenes.[31−33]

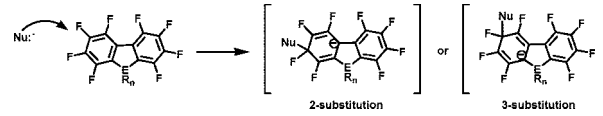

(1)

In these highly fluorinated systems ^{19}F NMR spectroscopy is a useful diagnostic tool, and valuable information is obtained from the fluorine chemical shifts and the F−F coupling constants. The chemical shift for a given fluorine atom (relative to C_6F_6) appears further downfield as the number of neighboring fluorine atoms is reduced. Additionally, very large through-bond F−F coupling (ranging from 75−175 Hz) can be observed between inequivalent fluorine atoms located near one another in space, even if they are 4 or 5 bonds apart.[34−39] In the work described here, this type of large coupling (100−160 Hz) is observed between fluorine atoms in the 4 and 5 positions of the monosubstituted heptafluoroheterofluorene intermediates that lead to the final disubstituted products (readily observed by monitoring the reactions by ^{19}F NMR spectroscopy). Observation of this F−F coupling for all monosubstituted products indicates that substitution never occurs in the 4 position. This is consistent with the fact that previously reported nucleophilic aromatic substitutions on **P′-F** and **S-F**, with oxygen and nitrogen-based nucleophiles, occur exclusively in the 2-position.[33] The disubstitutions reported here primarily occur in the 2- and 7-positions, as indicated by characterizations of four examples by X-ray crystallography (vide infra). Indeed, substitutions in the 2- and 3-positions are expected to be favored, since the intermediates generated by attack at the 1- or

(26) (a) Cohen, S.; Fenton, D.; Tomlinson, A.; Massey, A. *J. Organomet. Chem.* **1966**, *6*, 301. (b) Cohen, S.; Massey, A. *J. Organomet. Chem.* **1967**, *10*, 471.

(27) Chambers, R. D.; Spring, D. J. *J. Fluorine Chem.* **1971/72**, *1*, 309.

(28) Chambers, R.; Cunningham, J.; Spring, D. J. *Tetraherdron* **1968**, *24*, 3997.

(29) (a) Burdon, J. *Tetrahedron* **1965**, *21*, 3373. (b) Wang, Y.; Watson, M. D. *J. Am. Chem. Soc.* **2006**, *128*, 2536. (c) Ding, J.; Day, M. *Macromolecules* **2006**, *39*, 6054.

(30) Zimmerman, H. *Tetrahedron* **1961**, *16*, 169.

(31) Burdon, J. *Tetrahedron* **1965**, *21*, 3373.

(32) Burdon, J.; Parsons, I. *J. Am. Chem. Soc.* **1977**, *99*, 7445.

(33) (a) Chambers, R. D.; Spring, D. J. *Tetrahedron* **1971**, *1*, 669. (b) Burdon, J.; Kane, B. L.; Tatlow, J. C. *J. Fluorine Chem.* **1971/72**, *1*, 185.

(34) Burdon, J.; Childs, A. C.; Parsons, I. W.; Tatlow, J. C. *J. Chem. Soc., Chem. Commun.* **1982**, *10*, 534.

(35) Bolton, R.; Sandall, J. *J. Chem. Soc., Perkin 2* **1978**, 746.

(36) Burdon, J.; Parsons, I.; Gill, H. *J. Chem. Soc., Perkin 1* **1979**, 1351.

(37) Burdon, J.; Gill, H.; Parsons, I.; Tatlow, J. *J. Chem. Soc., Perkin 1* **1980**, 1726.

(38) Matthews, R. *Org. Magn. Reson.* **1982**, *18*, 266.

(39) Servis, K.; Fang, K.-N. *J. Chem. Soc.* **1968**, 6712.

4-positions would result in high-energy $p_\pi - p_\pi$ repulsive interactions at the fluorine-substituted carbanion.[32,35−37] Additional structural information is derived from the ^{19}F chemical shifts, since a given fluorine atom experiences a downfield shift of between 15 and 30 ppm upon substitution of an adjacent fluorine atom by a carbon atom. Thus, the NMR data allow for assignment of the chemical shift for the fluorine atom in the 1-position (resulting from substitution at the neighboring 2-position) or the 4-position (resulting from substitution at the neighboring 3-position).[37]

The synthesis of phenyl-, thienyl-, and phenylethynyl-substituted hexafluorophosphafluorene oxide compounds is illustrated in Scheme 2. These procedures involved generation of the parent hexafluorophosphafluorenes as synthetic intermediates. Following aqueous workup, these species were oxidized by addition of aqueous H_2O_2, and the products were obtained in moderate to good yields after column chromatography. Compound **P′-F** was readily converted to the 2,7-disubstituted products by addition of the appropriate carbon nucleophile at −78 °C followed by slow warming to room temperature. Even the relatively less reactive lithium phenylacetylide was completely consumed over 10 h at room temperature (by ^{19}F NMR spectroscopy). Monitoring the formation of **P′-PE** allowed assignments for the mono- and disubstituted compounds (see the Supporting Information for details). The absence of strong F−F coupling for the most downfield shifted resonance suggests substitution in the 2-position of the monosubstituted product. This assignment is further substantiated by independent synthesis of **P′-PE** from 2,2′-dibromo-4,4′-di(phenylethynyl)-3,3′,5,5′,6,6′-hexafluorobiphenyl (vide infra), for which the substitution pattern of a derivative (**Sn-PE**) was established by X-ray crystallographic studies. For the thienyl derivative **P-Th**, the 2,7-substitution pattern was also confirmed by X-ray crystallography (vide infra).

Octafluorothiafluorene **S-F** and octafluorogermafluorene **Ge-F** were readily converted to the corresponding diphenyl- and dithienyl-substituted products via addition of the appropriate lithium reagent at −78 °C followed by slow warming to room temperature (Scheme 3). The analogous reactions with lithium phenylacetylide, to give **S-PE** and **Ge-PE**, required heating at 120 °C for at least 2 h. Isolated yields of the disubstituted phenyl and thienyl derivatives ranged from 50% to 80% but were only ∼30% for the phenylethynyl derivatives. The lower isolated yields for **S-PE** and **Ge-PE** are likely due to product loss during purification, resulting from inefficient separations from phenylethynyl-containing byproducts. Higher yields for both **S-PE** and **Ge-PE** were achieved when the heterofluorene was formed from 2,2′-dibromo-4,4′-di(phenylethynyl)-3,3′,5,5′,6,6′-hexafluorobiphenyl, as described in the following section. Monitoring the formation of **S-Ph** and **Ge-Ph** allowed assignments of ^{19}F NMR spectra for the mono- and disubstituted compounds (see the Supporting Information). The absence of strong F−F coupling for the most downfield shifted resonances suggests substitution in the 2-position of the monosubstituted product. The 2,7-substitution pattern for **Ge-Ph** was confirmed by a single-crystal X-ray analysis (vide infra). The 2,7 substitution patterns for **S-F** and **Ge-F** derivatives are further substantiated by independent synthesis of **S-PE** and **Ge-PE** from 2,2′-dibromo-4,4′-di(phenylethynyl)-3,3′,5,5′,6,6′-hexafluorobiphenyl (vide infra), for which the substitution pattern of a derivative (**Sn-PE**) was established by X-ray crystallographic studies.

Nucleophilic substitution on octafluorosilafluorenes **Si-F** and **Si′-F**, and octafluorostannafluorene **Sn-F**, occurred less readily and required more forcing conditions (Scheme 4). The reaction of **Sn-F** with a variety of nucleophiles predominantly resulted in decomposition, as indicated by the observation of 2,2′-dihydrooctafluorobiphenyl in the ^{19}F NMR spectra of crude reaction mixtures, suggesting nucleophilic attack at tin rather than on the aromatic ring. For the octafluorosilafluorenes the reaction yields and the position of substitution were found to be highly dependent on reaction conditions (solvent, nature of the nucleophile, etc.). It is unclear why these silicon and tin heterocycles are less well-behaved than the germanium analogue, but the more electropositive nature of these elements may render the fluorene derivative less electron deficient, and therefore less susceptible to nucleophilic attack. Also, silyl and stannyl groups are known to stabilize a negative charge on the adjacent carbon,[40] and this may lead to a reduction in 2,7-selectivity for nucleophilic attack. Overall, conversions to the disubstituted product and the 2,7-selectivities were much lower in polar solvents, as indicated by ^{19}F NMR spectra. The highest product yields were achieved with toluene or hexanes as the main solvent and a minimum amount of Et_2O required to solubilize the lithium reagent. Generally, the conversions and the selectivities for 2,7-substitution were increased when the silicon R′ substitutent was phenyl (vs methyl). While moderate yields of ∼50% were obtained for the phenyl (**Si-Ph**, **Si′-Ph**) and thienyl (**Si-Th**) derivatives, the di(phenylethynyl) analogues (**Si-PE**, **Si′-PE**) were not obtained by this method.

A superior synthetic route to 2,7-substituted di(phenylethynyl)silafluorene and di(phenylethynyl)stannafluorene compounds is based on 2,2′-dibromo-4,4′-di(phenylethynyl)-3,3′,5,5′,6,6′-hexafluorobiphenyl (**1**) as a starting material. This compound was synthesized via addition of 2.3 equiv of lithium phenyl acetylide to 2,2′-dibromooctafluorobiphenyl in THF (Scheme 5). Lithium−bromine exchange between **1** and BuLi in Et_2O/THF at −78 °C followed by addition of the appropriate dichlorosilane produced the desired silafluorene product in good yield (65% **Si′-PE**, 56% **Si-PE**). With this approach, it was possible to synthesize the corresponding 2,7-di(phenylethynyl)-substituted stannafluorene (**Sn-PE**, 71%), germafluorene (**Ge-PE**, 40%), thiafluorene (**S-PE**, 40%), and phosphafluorene oxide (**P-PE**, 55%) compounds. This strategy was not effective for preparing the phenyl- or thienyl-derivatives of the stannafluorene because lithium−bromine exchange between **1** and the nucleophile was favored over S_NAr_F. Single-crystal X-ray analyses for **Sn-PE** and **Si-Ph** (vide infra) confirmed the connectivity of **1** and the 2,7-substitution pattern for **Si-Ph**, respectively.

Spectroscopic Characterization of Fluorinated Heterofluorenes. The solution state UV−vis data collected for all compounds are summarized in Table 1. The corresponding HOMO−LUMO energy gaps (E_g^{opt}) were calculated from the absorption onset wavelength, which was taken to be the intersection of the leading edge tangent with the *x*-axis. UV−visible absorption behavior for the parent octafluoroheterofluorenes exhibit little to no dependence on the heteroatom, and HOMO−LUMO energy gaps are between 3.75 and 3.90 eV. Derivatizations of the heterofluorenes in the 2- and 7-positions lead to a red-shift in the absorption maximum, as illustrated in Figure 1 for phosphafluorene oxide derivatives **P-F**, **P-Ph**, **P-Th**, and **P-PE**. Compared to the parent compounds, the 2,7-diphenylhexafluoroheterofluorenes exhibit a slight red-

(40) Alt, H.; Franke, E. R.; Bock, H. *Angew. Chem., Int. Ed.* **1969**, *8*, 525.

TABLE 1. Selected Optical Characterization Data for Heterofluorenes

	λ_{abs}/nm (log ε)	E_g^{opt}/eV, soln	λ_{ems}/nm, soln	Φ_{PL}, soln	λ_{ems}/nm, solid
P-F	325(3.6)	3.7	365	0.18[a]	378
P-Ph	338(3.8)	3.4	395	0.60[a]	428
P-Th	385	3.0	424	0.54[b]	
	369		443		
P-PE	380(3.7)	3.1	414	0.98[b]	472
			432		
S-F	322(3.6)	3.75	364	<0.01[a]	
S-Ph	344(3.5)	3.8	369	0.03[a]	447
S-Th	336	3.3	380	0.27[b]	
	352		397		
S-PE	359(3.7)	3.3	392	0.08[b]	473
			404		
Ge-F	308(3.5)	3.9	331	0.03[a]	
Ge-Ph	315(4.1)	3.7	365	0.25[a]	406
Ge-Th	367(3.5)	3.2	395	0.80[b]	467−484
			415		
Ge-PE	368(4.6)	3.2	399	1.0[b]	467
			411		
Si′-F	307	3.9	337	0.20[a]	336
Si′-Ph	321(4.3)	3.6	369	0.70[a]	430449
Si′-PE	367(4.3)	3.2	389	1.0[a]	473
			402		
Si-F	315(3.6)	3.75	365	0.26[a]	378
Si-Ph	325(4.8)	3.7	376	0.70[a]	436457
Si-Th	358(4.5)	3.2	400	0.80[b]	450−477
			420		
Si-PE	354	3.2	392	1.0[b]	
			414		
Sn-F	309	3.95			
Sn-PE	363	3.2	389	0.65[b]	485
	350		410		

[a] Referenced to 1,4-bis-(5-phenyloxaole-2-yl)benzene (POPOP) in THF ($\Phi_{P\ L}$ = 0.97). [b] Referenced to 9,10-diphenylanthracene in THF (ΦP L = 0.9).

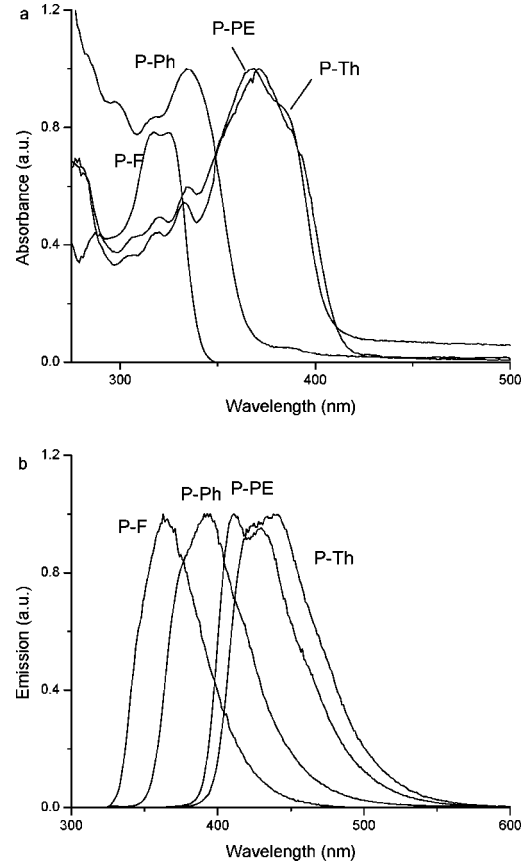

FIGURE 1. Solution state absorption (a) and emission (b) in THF for phosphafluorene oxide compounds **P-F**, **P-Ph**, **P-Th**, and **P-PE**.

shift, ca. 20 nm, in the absorption energies suggesting a minor extension of the conjugation length. Exchange of the phenyl groups for thienyl groups results in a significant red-shift in the absorption energies, and the HOMO−LUMO energy gaps drop by ca. 0.4 eV as compared to the parent and phenyl-substituted compounds. The phenylethynyl derivatives display HOMO−LUMO energy gaps that are similar to those of the thienyl analogues despite their potentially longer conjugation length, further illustrating that the nature of the substitutents is important in determining the electronic structure.

The effect of fluorination, which can stabilize both the HOMO and LUMO energy levels, on the absorption and emission behavior of organic compounds is often difficult to predict.[41] Examples of increases, decreases, and no change in HOMO−LUMO energy gaps for fluorinated (vs nonfluorinated) versions of the same compounds have been reported.[9,42] In this case, λ_{abs} values for the nonderivatized octafluoroheterofluorenes were similar to those of the analogous nonfluorinated heterofluorenes, suggesting that fluorination leads to comparable stabilization of both the HOMO and LUMO energy levels. Additionally, the 2,7-bis(phenylethynyl) derivatives possess E_g^{opt} values that are similar to those of the 2,7-bis(pentafluorophenylethynyl) derivatives, further illustrating a comparable stabilization in both the HOMO and LUMO energy levels.[24]

Solution state photoluminescence data for all compounds are summarized in Table 1. Emission energies were measured with 300 nm excitation wavelength light for parent octafluoroheterofluorene and phenyl-derivatized compounds, and with 350 nm excitation wavelength light for the thienyl and phenylethynyl derivatives. Derivatization of the heterofluorenes in the 2- and 7-positions leads to a red-shift in the emission energies consistent with the change in absorption energies described above, as illustrated in Figure 1 for phosphafluorene oxide derivatives **P-F**, **P-Ph**, **P-Th**, and **P-PE**. The energies of the emitted light (λ_{ems}) for these compounds exhibit a constant stokes shift of 25 to 30 nm from the absorption maximum, producing ultraviolet to violet light, and display little heteroatom dependence.

Dilute solution state (optical density 0.1) photoluminescence quantum yields (Φ_{PL}, Table 1) were determined for all compounds and it was found that the intensity of the emitted light (Φ_{PL}) varied widely across the series. These observations suggest that although the heteroatom does not seem to influence absorption or emission energies, there is significant HOMO and/or LUMO electron density located on the heteroatom, which can influence the intensities of these transitions. The observed decrease in Φ_{PL} values for the Group 14 derivatives, **Si′-F**, **Si-F** > **Ge-F** > **Sn-F**, may be explained by the heavy atom effect and the increase in intersystem crossing and nonradiative decay pathways with increasing principal quantum number.[43] The lower Φ_{PL} value for thiafluorene **S-F** versus phosphafluorene oxide **P-F** or silafluorenes **Si′-F** and **Si-F** may be explained by a more accessible triplet state or more nonradiative decay

(41) Matsuda, T.; Kadowaki, S.; Goya, T. *Org. Lett.* **2007**, *9*, 133–136.
(42) Medina, B.; Beljonne, D.; Egehaaf, H.-J.; Gierschner, J. *J. Chem. Phys.* **2007**, *126*, 111101.
(43) (a) Prodi, A.; Kleverlaan, C. J.; Indelli, M.; Scandola, F.; Alessio, E.; Iengo, E. *Inorg. Chem.* **2001**, *40*, 34–98. (b) Gutierrez, A.; Whitten. D. *J. Am. Chem. Soc.* **1976**, *98*, 6233. (c) Beljonne, D.; Shuai, Z.; Pourtois, G.; Bredas, J. L. *J. Phys. Chem. A* **2001**, *105*, 3899.

pathways due to the lone pairs of electrons on the sulfur atom. Indeed, it was observed that the unoxidized phosphafluorene **P-F′**, with one lone pair of electrons, exhibits a much lower Φ_{PL} value (not shown) than the oxidized phosphafluorene oxide.

Additionally, the nature of the 2,7-substituents has a significant effect on the emission intensities. The 2,7-diphenylhexafluoroheterofluorenes exhibit a significant increase in the Φ_{PL} value (3 times or more) versus the corresponding octafluoroheterofluorenes. Exchanging the phenyl groups for thienyl groups results in a moderate increase in Φ_{PL} for all compounds except the phosphafluorene oxide derivative (which demonstrates a slight decrease in emission intensity). All 2,7-di(phenylethynyl)hexafluoroheterofluorenes, except for thiafluorene **S-PE**, exhibit high Φ_{PL} values (>0.65), even approaching unity with the silafluorene- and phosphafluorene oxide-based systems. Similarly high Φ_{PL} values (~1) were also observed for the 2,7-bis(pentafluorophenylethynyl) derivatives.[24]

In the literature there are examples of both increases and decreases of Φ_{PL} values upon fluorination.[9,42] In this work a significant increase in emission intensity is observed for many of the octafluoroheterofluorenes when compared to their nonfluorinated counterparts.[16,41,42] Although optical properties for the nonfluorinated analogues of the 2,7- derivatized heterofluorenes have not been reported, polymers and oligomers containing silafluorene units are highly emissive; thus high Φ_{PL} values (>0.7) can be expected for these types of molecules.[41]

Despite the poor film-forming properties of these materials, which result in nonuniform layers by solution casting, it was possible to collect solid state emission data for a number of compounds (Table 1). The solid state emission energy ($\lambda_{ems,solid}$) for the parent compounds exhibits almost no change from those observed in solution. However, the $\lambda_{ems,solid}$ energies for the 2,7-derivatized compounds are red-shifted between 30 and 80 nm from the corresponding values in solution, which strongly suggests the existence of intermolecular electronic communication for these extended structures.

Electrochemical Studies on Fluorinated Heterofluorenes. The solution state redox behavior of all compounds was investigated via differential pulse voltammetry (reduction and oxidation potentials) and cyclic voltammetry (reversibility). The relevant results are summarized in Table 2. All measurements were performed in a CH_3CN electrolyte solution (0.1 M solution of tetrabutylammonium hexafluorophosphate in CH_3CN) with a $Ag/AgNO_3$ nonaqueous reference electrode and HOMO/LUMO energy levels were calculated with respect to the appropriate ferrocene−ferrocenium (Fc/Fc^+) oxidation or reduction (Fc HOMO energy of −4.8 eV relative to vacuum).[44] The LUMO energies range from −2.6 to −3.3 eV. The reversibility of the reduction varies throughout the entire series and representative cyclic voltammetry (CV) curves are shown in Figure 2. Oxidation behavior, when observed, is always irreversible and HOMO−LUMO energy gaps calculated from the electrochemical analysis are in good agreement with those calculated from the UV−vis data. In many cases, multiple reduction and oxidation events are observed and the details of these transitions are available in the Supporting Information.

TABLE 2. Selected Electrochemical Characterization Data for Perfluoroheterofluorenes

	LUMO[a]/eV	HOMO[a]/eV	E_g^{CV}/eV, soln	E_g^{opt}/eV, soln
P-F	−3.0[b]			3.7
P-Ph	−3.0[b]	−6.7	3.7	3.4
P-Th	−3.1[b]	−6.2	3.1	3.0
P-PE	−3.3[b,d]	−6.5	3.2	3.1
S-F	−2.5	−6.7	4.2	3.75
S-Ph	−2.7			3.8
S-Th	−2.8[c]	−6.1	3.3	3.3
S-PE	−3.0[c,d]	−6.4	3.4	3.3
Ge-F	−2.6			3.9
Ge-Ph	−2.7[b]	−6.3	3.6	3.7
Ge-Th	−2.8[b]	−6.1	3.3	3.2
Ge-PE	−3.0[b,d]	−6.4	3.4	3.2
Si′-F	−2.7			3.9
Si′-Ph	−2.6[c]	−6.5	3.9	3.6
Si′-PE	−3.0[c,d]	−6.4	3.4	3.2
Si-F	−2.6			3.75
Si-Ph	−2.7[b]	−6.5	3.8	3.7
Si-Th	−2.9[c]	−6.1	3.2	3.2
Si-PE	−3.0[d]			3.2
Sn-F	−2.6			3.95
Sn-PE	−2.8[d]			3.2

[a] Referenced to Fc/Fc^+ (HOMO energy level −4.8 eV below vacuum). [b] Reversible reduction. [c] Quasireversible reduction. [d] Three drops of toluene was added to improve solubility in CH_3CN.

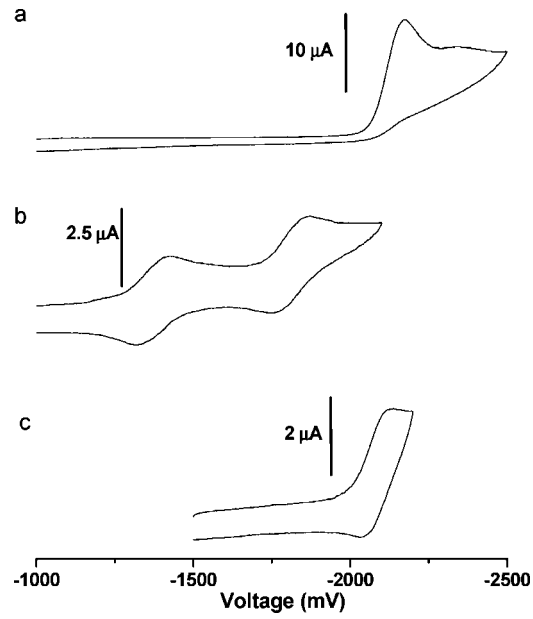

FIGURE 2. Representative cyclic voltammetry curves demonstrating the differences in reduction behavior: (a) irreversible reduction (**Ge-F**), (b) reversible reduction (**P-PE**), and (c) quasireversible reduction (**Si′-Ph**).

The LUMO energy values of −2.6 to −3.3 eV are significantly lower than those of the nonfluorinated heterofluorene compounds previously reported in the literature,[45−47] and slightly higher than those reported for the 2,7-bis(pentafluorophenylethynyl) derivatives (~0.2 eV).[24] This clearly illustrates the effect of fluorination in reducing the LUMO energy level and puts these small molecules in the range of a number of

(44) Koepp, H.; Wendt, H.; Strehlow, H. *Z. Elektrochem.* **1960**, *64*, 483.
(45) Huang, T.-H.; Whang, W.-T.; Shen, J. Y.; Wen, Y.-S.; Lin, J. T.; Ke, T.-H.; Chen, L.-Y.; Wu, C.-C. *Adv. Funct. Mater.* **2006**, *16*, 1449–1456.
(46) Chan, K. L.; McKiernan, M.; Towns, C.; Holmes, A. B. *J. Am. Chem. Soc.* **2005**, *127*, 7662–3.
(47) Mo, Y.; Tian, R.; Shi, W.; Cao, Y. *Chem. Commun.* **2005**, 4925.

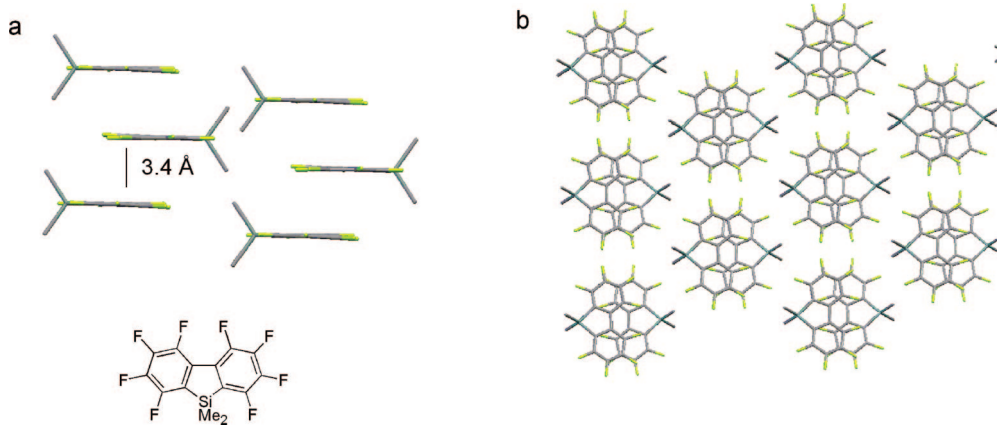

FIGURE 3. Crystal structure for silafluorene **Si′-F**: (a) view perpendicular to the stacking direction and (b) view parallel to the stacking direction illustrating the hexagonal packing of individual π-stacked columns. Hydrogen atoms have been removed for clarity.

useful n-type conducting materials.[4,12,48] The LUMO levels for the parent octafluoroheterofluorenes are all around −2.7 eV, except for phosphafluorene oxide **P-F** which possesses a slightly lower LUMO level at −3.0 eV. Additionally, **P-F** was the only nonderivatized heterofluorene to exhibit reversible reduction behavior. Phenyl substitution in the 2- and 7-positions does little to alter the LUMO energy level, although it does increase the reversibility of the radical anion formation for the silafluorene and germafluorene compounds. The thienyl and phenylethynyl derivatives exhibit significantly lower LUMO energy levels, a decrease of about 0.2−0.3 eV versus those of the parent compounds, which is to be expected due to their slightly longer conjugation length. The thienyl derivatives maintain some of the reversibility observed for the phenyl derivatives, although small amounts of electropolymerization at the Pt working electrode was observed. This electropolymerization could likely be prevented by capping the 5-position on the terminal thiophenes and may improve the reversibility of the electrochemical transitions. The thienyl derivatives exhibit higher HOMO energy levels than the phenylethynyl derivatives, which would explain the similarities in their E_g^{opt} values despite their differences in conjugation length. Of the phenylethynyl derivatives, only the phosphafluorene oxide **P-PE** exhibits completely reversible reduction behavior. All other bis(phenylethynyl) compounds exhibit quasireversible or irreversible reductions. The reason for the poor reversibility of these compounds is unclear but could possibly be improved by the use of a more electron deficient aryl moiety, or by the use of a better solvent in the supporting electrolyte solution.

Solid State Structures of Fluorinated Heterofluorenes. While it would be preferable to demonstrate electron transport in these materials via the construction of a functioning device (e.g., FET, OLED, etc.), numerous attempts to solution cast these compounds failed to produce uniform films. However, single-crystal X-ray analysis of representative samples provides a means for investigating intermolecular interactions in the solid state. Since close cofacial intermolecular packing is desirable for many electronic applications, it is important to assess how molecular-level modifications influence the solid state assembly in these systems. Singly-crystal X-ray analyses of 2,7-bis(pentafluorophenylethynyl)hexafluorogermafluorene and -phosphafluorene oxide derivatives have shown that these compounds exhibit very planar π systems with parallel heterofluorene fragments;[24] however, the current study allows for a more extensive investigation into the influence of 2,7 functional groups and the heteroatom on packing in the solids state.

Examination of the solid state structures of the octafluoroheterofluorenes and 2,7-derivatized hexafluoroheterofluorenes illustrates the tendency for heterofluorenes to pack via the formation of cofacial intermolecular interactions, and the significant influence of small changes in molecular structure on the long-range intermolecular order. Additionally, the crystal structures of **Si-Ph**, **Ge-Ph**, **P-Th**, and **Sn-PE** confirm the 2,7-substitution positions inferred from the ^{19}F NMR spectroscopic data. Full crystallographic information on all X-ray structures is available in the Supporting Information.

All of the crystal structures involve cofacial intermolecular $\pi-\pi$ interactions with heterofluorene−heterofluorene distances ranging from 3.2 to 3.7 Å. This cofacial packing is typical of highly fluorinated aromatic systems,[23] whereas the less desired herringbone structure is observed for many of the nonfluorinated fluorene compounds.[19−21] The specific interfluorene spacing, as well as the extent of the π-system overlap, is influenced by both the heteroatom substituent and the 2,7-substituents. The influence of the heteroatom substituent can be illustrated by a comparison of the structures of octafluorosilafluorenes **Si′-F** and **Si-F** (Figures 3 and 4). While both structures exhibit cofacial stacking, the silafluorene with methyl groups on the silicon, **Si′-F**, stacks in hexagonally arranged columns (Figure 3) and exhibits appreciable π-stacking throughout the entire crystal. The silafluorene with phenyl substituents on the silicon, **Si-F**, pack in two nearly perpendicular directions and significant fluorene−fluorene π-interaction (3.4 Å) in a given direction occurs only between pairs of molecules which are offset from an optimal π-stacking direction and are separated by >3.6 Å.

Comparison of the structures of octafluorostannafluorene, **Sn-F**, and 2,7-di(phenylethynyl)hexafluorostannafluorene, **Sn-PE**, clearly illustrates the effect of 2,7-derivatizations on the solid state packing (Figures 5 and 6). As shown in Figure 5, **Sn-F** adopts a packing motif similar to that observed for **Si-F**, with the molecules aligned in two nearly perpendicular directions, and cofacial fluorene−fluorene π-overlap is much less significant between pairs of molecules. A very different packing arrangement is exhibited by 2,7-di(phenylethynyl)hexafluorostannafluorene, **Sn-PE**, which exhibits unidirectional π-stacking throughout the crystal (Figure 6).

(48) Lee, B. L.; Yamamoto, T. *Macromolecules* **1999**, *32*, 1375–1382.

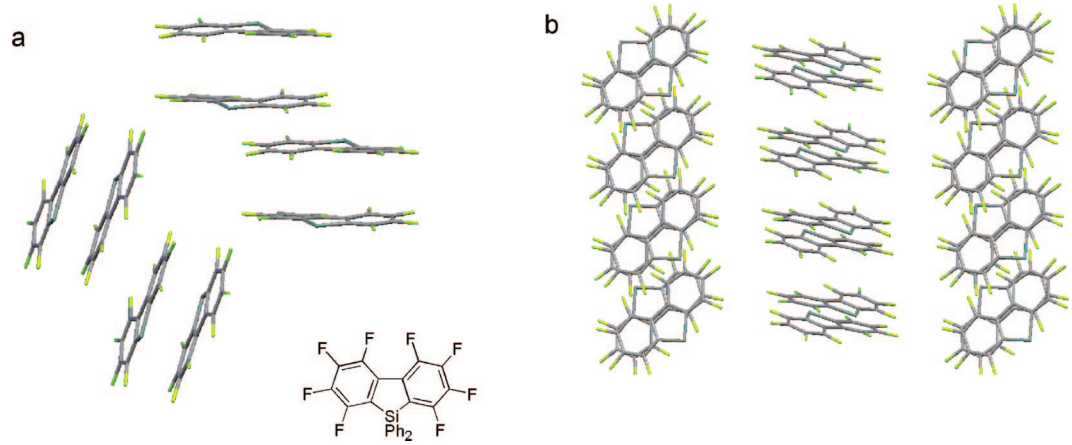

FIGURE 4. Crystal structure for silafluorene **Si-F**: (a) view illustrating π-interactions between molecules and (b) view illustrating the lateral offset between pairs of molecules. Hydrogen atoms and Si-phenyl groups have been removed for clarity.

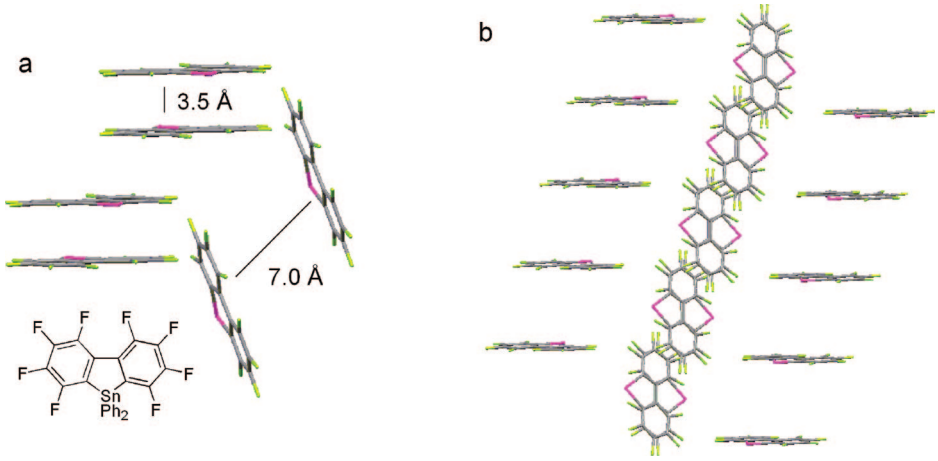

FIGURE 5. Crystal structure for stannafluorene **Sn-F**: (a) view illustrating cofacial interactions and (b) view illustrating the offset between the pairs of π-stacked molecules. Hydrogen atoms and Sn-phenyl groups have been removed for clarity.

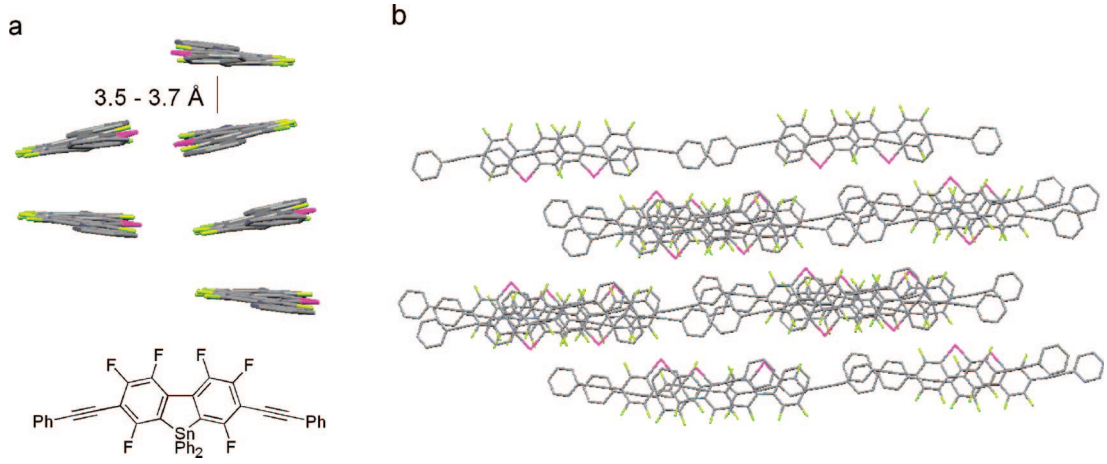

FIGURE 6. Crystal structure for stannafluorene **Sn-PE**. (a) view perpendicular to the stacking direction and (b) view parallel to the stacking direction, illustrating the continuous π-overlap. Hydrogen atoms and Sn-phenyl groups have been removed for clarity.

The presence of thienyl groups (**P-Th**) instead of phenyl groups (**Ge-Ph**), as illustrated in Figures 7 and 8 results in a much more planar aryl−fluorene−aryl ring system. For **P-Th** (Figure 7) the torsion angles between the fluorene core and the thiophenes rings are 7° and 25° versus torsion angles of ∼50° between the 2,7-phenyl rings and the fluorene core for **Ge-Ph** (Figure 8). Even though the molecules in **P-Th** pack in one direction throughout the crystal and the molecules in **Ge-Ph** pack in two nearly perpendicular directions, both systems exhibit a similar "slip" away from a π-stacked column, with close $\pi-\pi$ interactions occurring only for pairs of molecules. It is possible that slightly less bulky groups on the heteroatoms would result in a more continuous π-system overlap, especially for the more planar thienyl derivatives.

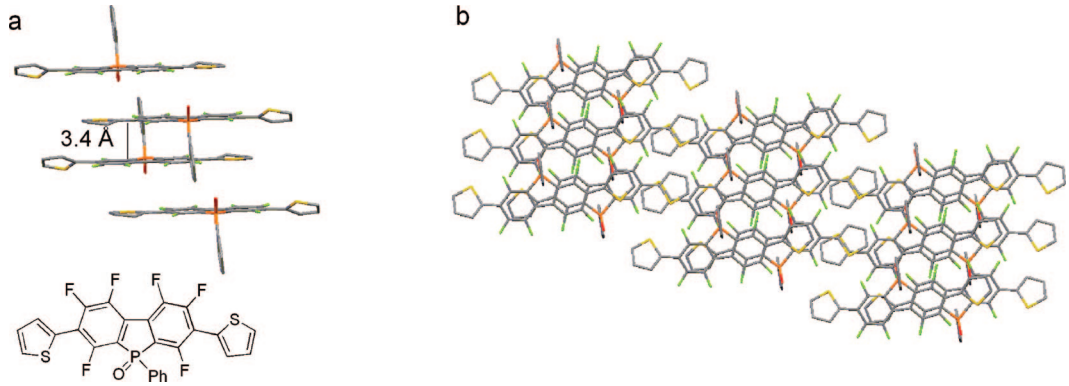

FIGURE 7. Crystal structure for 2,7-dithienylperfluorophosphafluorene oxide **P-Th**. (a) view illustrating π-interactions between molecules and (b) view illustrating the lateral offset between pairs of molecules. Hydrogen atoms have been removed for clarity.

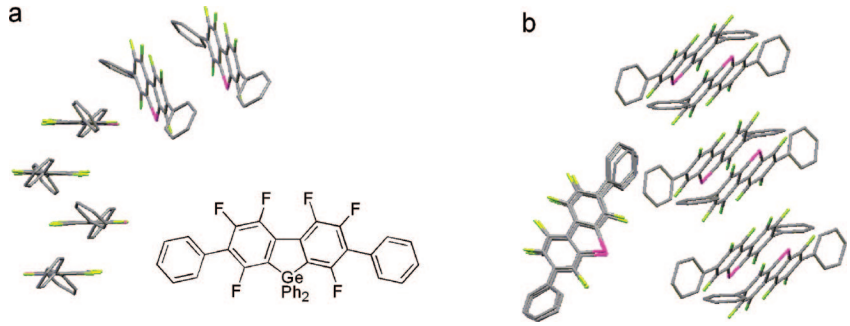

FIGURE 8. Crystal structure for 2,7-diphenylgermafluorene **Ge-Ph**: (a) view illustrating cofacial interactions between molecules and (b) view illustrating the offset between pairs of molecules. Hydrogen atoms and Ge-phenyl groups have been removed for clarity.

Concluding Remarks

A series of 2,7-substituted hexafluoroheterofluorenes has been prepared via nucleophilic aromatic substitution, and their optical, electrochemical, and solid state packing properties have been investigated. The synthesis and characterization of these compounds builds upon the previous work in our laboratories on the evaluation of such materials as n-type components with potential electronic applications (n-type FETs, OLED and PV electron transport layers, etc.).[24] The silafluorene and phosphafluorene oxide derivatives exhibit very intense, high-energy emissions, making them interesting candidates for devices based on electro- and photoluminescence. The low LUMO energies and cofacial solid state packing observed for many of these compounds suggest that they may function well as building blocks for electron transporting materials. In this respect, it is worth noting that changes in the heteroatom substituents influence the nature of crystal packing, without significantly altering electronic properties. Thus, these systems may be synthetically tunable such that electronic and solid state properties may be independently varied. Unfortunately the poor film-forming and adhesion properties of the compounds in this study prevented studies on electron transport in the solid state. Current work is focused on addressing these problems through modifications of the structures of these fluorinated heterofluorene molecules via the incorporation of various substituents.

Experimental Section

There are literature procedures for the synthesis of 9-phenyloctafluorophosphafluorene and the underivatized octofluoroheterofluorenes (**Si′-F**, **Si-F**, **P-F**, **S-F**, **Ge-F**, **Sn-F**) and the changes made to the synthesis and purification to improve yields are described in the Supporting Information. Additionally the synthesis, isolation, and characterization of **P-F′**, **P-Th**, **S-Th**, **S-PE**, **Si-Ph**, **Si-Th**, **Si-PE**, **Si′-Ph**, **Si′-PE**, and **Sn-PE** is described in the Supporting Information.

2,7,9-Triphenylhexafluorophosphafluorene Oxide (P-Ph). To a solution of **P-F′** (0.100 g, 0.25 mmol) in toluene (2 mL) at −78 °C was added a solution of phenyllithium (0.052 g, 0.62 mmol) in Et_2O (1.5 mL). The mixture was allowed to warm to room temperature over 12 h with stirring. The resulting light yellow solution was quenched with water (10 mL) and the organic components were extracted into toluene (2 × 5 mL). The combined extracts were dried over $MgSO_4$ and concentrated via rotary evaporation. The resulting solid was dissolved in CH_2Cl_2 (30 mL) and then H_2O_2 (0.1 mL, 30 wt % solution in H_2O) was added and the resulting mixture was stirred for 4 h. The reaction mixture was washed with water (2 × 15 mL) and the organic components were dried over $MgSO_4$, filtered through Celite, and concentrated via rotary evaporation. The disubstituted product was isolated via slow evaporation of hot hexanes/CH_2Cl_2 to give 0.034 g (0.07 mmol, 25% yield) of **P-Ph** as a tan powder. ^{1}H ($CDCl_3$, 400 MHz, 25 °C) δ 7.48 (12H, m), 7.61 (1H, m), 7.79 (2H, m); ^{19}F NMR ($CDCl_3$, 376 MHz, 25 °C) δ −112.21 (1F, m), −126.71 (1F, m), −132.93 (1F, m); ^{31}P ($CDCl_3$, 161.9 MHz, 25 °C) δ 28.12 (s). MS 520 (M^+) 443. Anal. Calcd for $C_{30}H_{15}F_6OP$: C, 67.17; H, 2.82. Found: C, 67.11; H, 3.18. Mp 265−267 °C dec.

2,7-Bis(phenylethynyl)-9-phenylhexafluorophosphafluorene Oxide (P-PE). Method 1: To a solution of **P-F′** (0.050 g, 0.12 mmol) in toluene (2 mL) at −78 °C was added a solution of lithium phenylacetylene (0.040 g, 0.36 mmol) in THF (2 mL). The mixture was allowed to warm to room temperature over 12 h with stirring. The resulting yellow solution was quenched with water (30 mL) and the organic components were extracted into toluene (2 × 10 mL). The extracts were dried over $MgSO_4$, filtered through celite, and concentrated via rotary evaporation. The resulting solid was dissolved in CH_2Cl_2 (15 mL) and then H_2O_2 (0.1 mL, 30 wt % solution in H_2O) was added and the resulting solution was stirred over 4 h. The reaction mixture was quenched with water (2 × 15

mL) and the organic components were dried over $MgSO_4$, filtered through Celite, and concentrated via rotary evaporation. The disubstituted product was isolated via slow evaporation of CH_2Cl_2:hex to give 0.035 g (0.06 mmol, 50% yield) of **P-PE** as a bright yellow powder.

Method 2: 2,2′-Dibromo-4,4′-bis(phenylethynyl)hexafluorobiphenyl (0.030 g, 0.05 mmol) was dissolved in toluene/THF (10 mL/ 2 mL) and the resulting solution was cooled to − 78 °C. To this was added butyllithium (0.06 mL, 1.6 M in hexanes) and the solution was mixed for 2 h at −78 °C. In a separate Schlenk flask dichlorophenylphosphine (0.05 mL) was added to dry THF (1 mL) and this mixture was deoxygenated via two series of freeze/pump/thaw cycles. The dichlorophenylphosphine solution was added to the cooled dilithio solution and the resulting mixture was warmed to room temperature over 8 h with stirring. The resulting yellow solution was quenched with water (10 mL) and the organic components were extracted into CH_2Cl_2 (2 × 10 mL). The combined extracts were dried over $MgSO_4$, filtered through Celite, and concentrated via rotary evaporation. The resulting solid was dissolved in CH_2Cl_2 (10 mL) and then H_2O_2 (0.1 mL, 30 wt % solution in H_2O) was added and the resulting solution was stirred for 4 h. The reaction mixture was quenched with water (2 × 15 mL) and the organic components were dried over $MgSO_4$, filtered through Celite, and concentrated via rotary evaporation. The disubstituted product was isolated via washing with acetone to give 0.015 g (0.03 mmol, 55% yield) of **P-PE** as a bright yellow powder.

^{1}H ($CDCl_3$, 400 MHz, 25 °C) δ 7.40 (6H, m), 7.53 (1H, m), 7.55 (4H, m), 7.64 (2H, m), 7.78 (2H, m); ^{19}F NMR ($CDCl_3$, 376 MHz, 25 °C) δ −105.94 (1F, m), −120.04 (1F, m), −132.89 (1F, m); ^{31}P ($CDCl_3$, 161.9 MHz, 25 °C) δ 28.47 (s). Anal. Calcd for $C_{34}H_{15}F_6OP$: C, 69.87; H, 2.59. Found: C, 69.97; H, 2.58. Mp 285−290 °C dec.

2,7-Diphenylhexafluorothiafluorene (S-Ph). To a solution of **S-F** (0.022 g, 0.07 mmol) in toluene (2 mL) at −78 °C was added a solution of phenyllithium (0.028 g, 0.33 mmol) in Et_2O (1.5 mL). The resulting mixture was allowed to warm to room temperature over 12 h with stirring. The resulting light yellow solution was quenched with water (15 mL) and the organic components were extracted into toluene (2 × 10 mL). The combined extracts were dried over $MgSO_4$, filtered through Celite, and concentrated via rotary evaporation. The disubstituted product was isolated via recrystallization from hot hexanes to give 0.024 g (0.06 mmol, 80% yield) of **S-Ph** as a white powder. ^{1}H ($CDCl_3$, 400 MHz, 25 °C) δ 7.50−7.60 (m); ^{19}F NMR ($CDCl_3$, 376 MHz, 25 °C) δ −120.92 (1F, m), −136.78 (1F, m), −141.47 (1F, m). MS 444 (M^+). Anal. Calcd for $C_{24}H_{10}F_6S$: C, 64.87; H, 2.27; S, 7.22. Found: C, 64.81; H, 1.97; S, 6.98. Mp 235−237 °C dec.

2,7-Bis(phenylethynyl)hexafluorothiafluorene (S-PE). Method 1: Octafluorothiafluorene (0.100 g, 0.3 mmol) and lithium phenylacetylene (0.145 g, 1.4 mmol) were dissolved in toluene (2 mL) and THF (0.5 mL). The resulting solution was heated, with stirring, at 90 °C for 8 h. The resulting brown solution was quenched with water (15 mL) and the organic components were extracted into toluene (2 × 15 mL). The combined extracts were dried over $MgSO_4$, filtered through Celite, and concentrated via rotary evaporation. The resulting solid was dissolved in CH_2Cl_2, absorbed onto alumina, and passed through an alumina plug (hexanes:CH_2Cl_2 10:1). The disubstituted product was isolated via slow evaporation of CH_2Cl_2 from a hexanes/CH_2Cl_2 mixture to give 0.035 g (0.7 mmol, 24% yield) of **S-PE** as a yellow powder.

Method 2: 2,2′-Dibromo-4,4′-bis(phenylethynyl)hexafluorobiphenyl (0.050 g, 0.08 mmol) was dissolved in Et_2O/THF (7 mL/2 mL) and the resulting solution was cooled to −78 °C. To this was added butyllithium (0.1 mL, 1.6 M in hexanes) and the resulting solution was stirred for 2 h at −78 °C. In a separate Schlenk flask sulfur monochloride (0.5 mL) was added to dry THF (2 mL) and this mixture was deoxygenated via two series of freeze/pump/thaw cycles. The sulfur monochloride solution was added to the cooled dilithio solution and the resulting mixture was warmed to room temperature over 8 h with stirring. The resulting yellow solution was quenched with water (20 mL) and the organic components were extracted into CH_2Cl_2 (2 × 20 mL). The combined extracts were dried over $MgSO_4$ and concentrated via rotary evaporation. The disubstituted product was isolated via slow evaporation of CH_2Cl_2 from a hexanes/CH_2Cl_2 mixture to give 0.016 g (0.03 mmol, 40% yield) of **S-PE** as a yellow powder.

^{1}H ($CDCl_3$, 400 MHz, 25 °C) δ 7.43 (3H, m), 7.65 (2H, m); ^{19}F NMR ($CDCl_3$, 376 MHz, 25 °C) δ −114.06 (1F, m), −135.01 (1F, m), −136.51 (1F, m). Anal. Calcd for $C_{28}H_{10}F_6S$: C, 68.29; H, 2.05. Found: C, 68.17; H, 1.92. Mp 245 °C dec.

2,2′-Dibromo-4,4′-bis(phenylethynyl)hexafluorobiphenyl (1). To a solution of 2,2′-dibromooctafluorobiphenyl (0.535 g, 1.2 mmol) in THF (75 mL) was added a solution of lithium phenylacetylene (0.290 g, 2.8 mmol) in THF (10 mL) and the resulting solution was stirred for 16 h. The resulting yellow solution was quenched with water (20 mL) and the organic components were extracted into CH_2Cl_2 (2 × 20 mL). The combined extracts were dried over $MgSO_4$, filtered through celite, and concentrated via rotary evaporation. The disubstituted product was isolated via column chromatography (hexanes on alumina) to give 0.400 g (55%, 0.66 mmol) of **1** as a white powder. ^{1}H ($CDCl_3$, 400 MHz, 25 °C) δ 7.42 (3H, m), 7.62 (2H, m); ^{19}F NMR ($CDCl_3$, 376 MHz, 25 °C) δ −103.28 (1F, m), −131.24 (1F, m), −137.80 (1F, m). MS 620 (M^+), 460, 310. Anal. Calcd for $C_{28}H_{10}Br_2F_6$: C, 54.23; H, 1.63. Found: C, 53.95; H, 1.60. Mp 213−215 °C.

Acknowledgment. This work was supported by the National Science Foundation research grant CHE0314709 and the DuPont Center for Collaborative Research and Education.

Supporting Information Available: Full experimental details, NMR data for determination of substitution patterns, and crystallographic data for **Si′-F**, **Si-F**, **Si-Ph**, **Ge-F**, **Ge-Ph**, **P-Th**, and **Sn-PE**. This material is available free of charge via the Internet at http://pubs.acs.org.

JO802171T